Supporting Information

Oancea et al. 10.1073/pnas.0811260106

SI Materials and Methods

Sequence Alignment and Secondary Structure Prediction. The quality of a homology model is governed directly by the accuracy of the sequence alignment. In low sequence identity regions such as the transmembrane domain (TMD), an inaccurate sequence alignment potentially alters the residue distribution of the translocation pore and the interhelical contact points that enable functional regions of TAP1/2 to be identified from the homology model. Secondary structure predictions were previously performed on TAP1 and TAP2 to pin down the location of membrane spanning helices (1), improving the quality of the sequence alignment in this region. The Sav1866 crystal structure contains 15 helical segments in the TMD alone, arranged into 6 transmembrane helices that extend up to 35 Å into the cytoplasm, coupling with the nucleotide-binding domains (NBDs) (2). To demarcate the membrane embedded regions of each helix, secondary structure predictions were performed on the Sav1866 primary sequences using 4 different transmembrane helix (TM) prediction servers (SOSUI, TMHMM, TopPRED2, and TMpred) (3–6). To verify the secondary structure predictions, the membrane spanning regions of the Sav1866 were also identified from a 1-palmitoyl-2-oleoyl-*sn*-glycero-3-phosphoethanolamine (POPE) embedded, solvated, and equilibrated Sav1866 crystal structure (PDB ID code 2HYD). These were compared to the TAP1 and TAP2 secondary structure predictions and experimentally determined membrane-spanning segments (1). Although the predictions do not precisely concur with the experimental predictions, the experimental TAP1/2 and modeled Sav1866 helix demarcations concur, and the location of the predicted TM helices correlated with the secondary structure alignment, increasing our confidence in the TMD sequence alignment.

Construction and Expression of Mutants. Single cysteine TAP1 mutants of cytosolic loop 1 (CL1) (T273C, E274C, F275C, Q278C, and N279C) and of CL2 (I368C, E369C, A370C, P375C, T376C, V377C, R378C, S379C, F380C, A381C, and N382C) were generated by ligase chain reaction with the following primers using Cys-less human TAP1 with a C-terminal His_{10}-tag as template (1): T273C, CGTCCTGAGACAGGAATGCGAATTCTTCCA; E274C, GACAGGAAACCTGCTTCTTCCAGCAGAAC; F275C, AACCGAATTCTGCCAGCAGAACCAGAC; Q278C, GAATTCTTCCAGTGCAACCAGACCGGCAACAT; N279C, TTCTTCCAGCAGTGCCAGACCGGCAACAT; I368C, CCCAGGTCGCTTGCGAAGCCTTAAGTG; E369C, CAGGTCGCTATCTGCGCCTTAAGTGCTA; A370C, GGTCGCTATC GAATGCTTAAGTGCTATGCC; P375C, GCCTTAAGTGCTATGTGTACCGTCAGATC C; T376C, GTGCTATGCCTTGCGTCAGATCCTTC; V377C, TGCTATGCCTACCTGC AGATCCTTCGCTAA; R378C, TATGCCTACCGTCTGCTCCTTCGCTA AC; S379C, CCTACCGTCAGATGCTTCGCTAACGAAGA; F380C, TACCGTCAGATCCTGCGCT AACGAAGAAG; A381C, CAGATCCTTCTGTAACGAAGAAGGCGAAGCTC; N382C, AGATCCTTCGCTTGCGAAGAGGCGAAGCTC (exchanged nucleotides are underlined). The single cysteine TAP1 mutants Q277C, G282C, N283C, I284C, M285C, S286C, R287C, and V288C were generated by ligase chain reaction as described (7). The single cysteine TAP1 mutants of the CL1 were cloned in the BspTI and MluI sites of pFastBac1_TAP1(Cys-less), whereas the single-cysteine TAP1 mutants of the CL2 were cloned in the SphI and StuI sites of pFastBac1_TAP1(Cys-less). The conserved E602 in the X-loop of TAP2 was mutated by ligase chain reaction with the following primers using single-cysteine TAP2(C213) as template: E602C, TACACCGATGTCGGCTGCAAGGGCTCCCAACTG; E602R, CCGAT GTCGGCAGAAAGGGCTCCCAACT; E602D, CCGATGTCGGCGATAAGGGCTCCCA ACT; E602A, TACACCGATGTCGGCGCTAAGGGCTCCCAACT. The X-loop mutants of TAP2 were cloned in the AjiI and AatII sites of pFasBac1-TAP2(C213). All enzymes for cloning were purchased from Fermentas. The constructs were confirmed by DNA sequencing. Baculovirus generation, virus infection, and protein expression were performed as previously described (8). Coinfections with baculoviruses containing single-cysteine TAP1 mutants and single-cysteine TAP2 (X-loop) were performed with a multiplicity of infection of 5. Infections with baculovirus containing Cys-less TAP1 in combination with Cys-depleted TAP2 were performed at a multiplicity of infection of 3 (1). TAP-containing membranes were prepared as previously described (7). The protein concentration was determined by the MicroBCA assay (Pierce).

Peptide Binding Assay. Peptides were radiolabeled with iodine (^{125}I) (8). TAP-containing membranes (25 μg of total protein) were incubated with 1 μM of radio-labeled peptide RRYQKSTEL in 50 μl of binding buffer (5 mM $MgCl_2$ in PBS, pH 7.4) for 15 min at 4 °C. Unbound peptides were removed by washing the membranes twice with 100 μl of ice-cold binding buffer using a vacuum manifold with 96-well filter plates (0.65 μm of polyvinylidene difluoride membranes, MultiScreen; Millipore). Membrane-associated radioactivity was quantified by γ-counting. Background binding was determined in the presence of 200-fold excess of unlabeled peptide (RRYQKSTEL).

Peptide Transport Assay. TAP-containing membranes (150 μg of total protein) were resuspended in 50 μl of binding buffer in the presence of 3 mM ATP or 2 units of apyrase. The transport reaction (50 μl) was started by adding 1 μM of fluorescent peptide RRYQNSTC$^{(F)}$L [$^{(F)}$, fluorescein-labeled cysteine] for 5 min at 32 °C and terminated with stop buffer (10 mM EDTA in PBS, pH 7.4) on ice (9). After centrifugation, the membranes were solubilized in lysis buffer (50 mM Tris/HCl, 150 mM NaCl, 5 mM KCl, 1 mM $CaCl_2$, 1 mM $MnCl_2$, 1% Nonidet P-40, pH 7.4) for 20 min on ice. N-core glycosylated, and therefore transported peptides were recovered overnight at 4 °C with Con A Sepharose beads (Sigma). After washing with lysis buffer, glycosylated peptides were eluted with 200 mM methyl-α-D-mannopyranoside (Sigma) in lysis buffer and quantified with a fluorescence plate reader ($\lambda_{ex/em}$ = 485/520 nm, Polarstar Galaxy; BMG Labtech).

1. Schrodt S, Koch J, Tampé R (2006) Membrane topology of the transporter associated with antigen processing (TAP1) within an assembled functional peptide-loading complex. *J Biol Chem* 281:6455–6462.
2. Dawson RJ, Locher KP (2006) Structure of a bacterial multidrug ABC transporter. *Nature* 443:180–185.
3. Hirokawa T, Boon-Chieng S, Mitaku S (1998) SOSUI: classification and secondary structure prediction system for membrane proteins. *Bioinformatics* 14:378–379.
4. Krogh A, Larsson B, von Heijne G, Sonnhammer EL (2001) Predicting transmembrane protein topology with a hidden Markov model: Application to complete genomes. *J Mol Biol* 305:567–580.

5. von Heijne G (1992) Membrane protein structure prediction. Hydrophobicity analysis and the positive-inside rule. *J Mol Biol* 225:487–494.
6. Hofmann K, Stoffel W (1993) TMbase - A database of membrane spanning proteins segments. *Biol Chem Hoppe-Seyler* 374:166–166.
7. Herget M, et al. (2007) Mechanism of substrate sensing and signal transmission within an ABC transporter: Use of a Trojan horse strategy. *J Biol Chem* 282:3871–3880.
8. Chen M, Abele R, Tampé R (2003) Peptides induce ATP hydrolysis at both subunits of the transporter associated with antigen processing. *J Biol Chem* 278:29686–29692.
9. Neumann L, Tampé R (1999) Kinetic analysis of peptide binding to the TAP transport complex: Evidence for structural rearrangements induced by substrate binding. *J Mol Biol* 294:1203–1213.

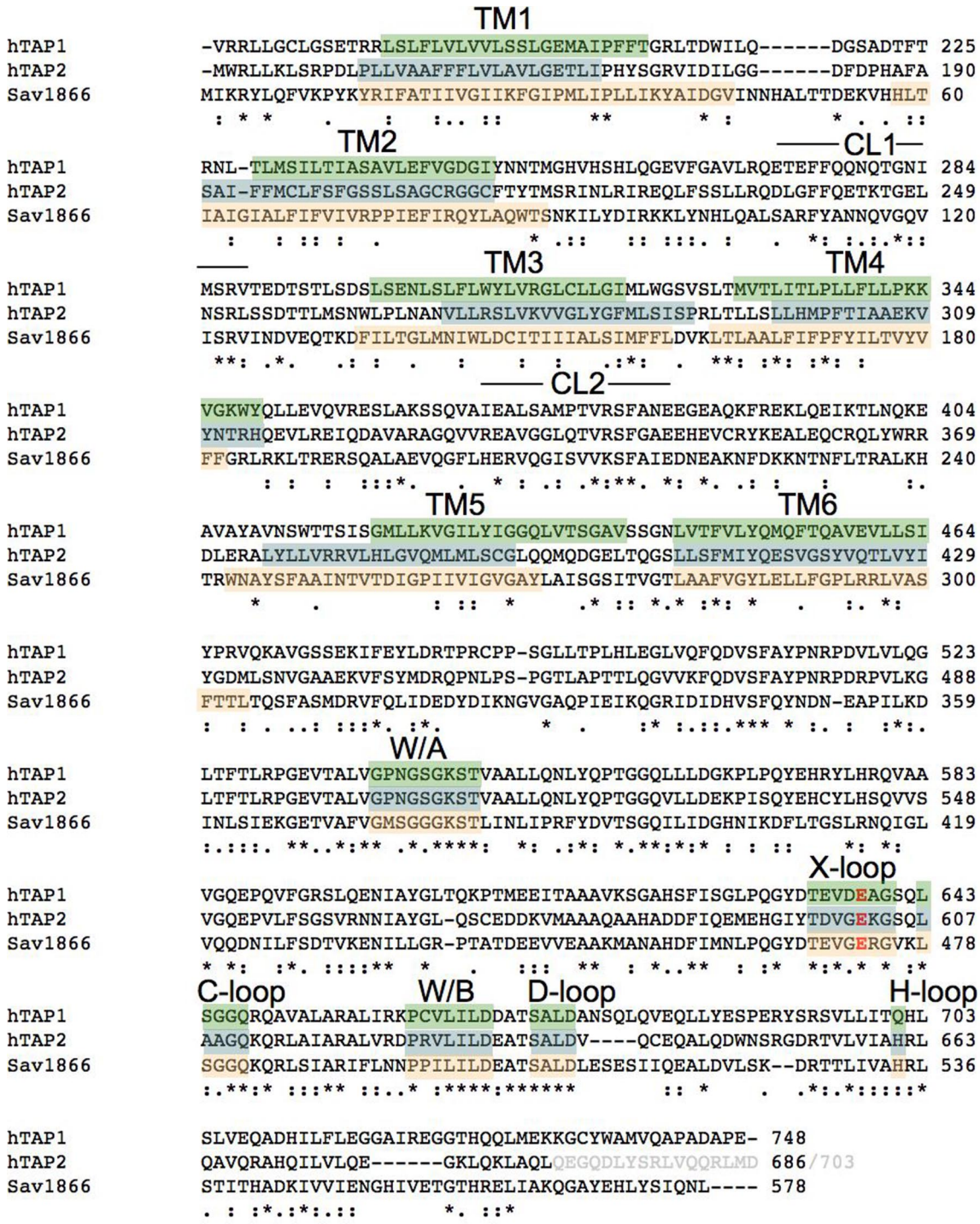

Fig. S1. Sequence alignment, membrane topology, and structural organization of TAP1, TAP2, and Sav1866. ClustalW2 was used for sequence alignment of human TAP1 (PDB ID code gi:45181465), TAP2 (PDB ID code gi:34638), and Sav1866 (PDB ID code gi:15924856). To verify the secondary structure predictions, the TM regions of the Sav1866 (orange) were also identified from a POPE embedded, solvated, and equilibrated Sav1866 structure (PDB ID code 2HYD) (2). These were compared to the TAP1 and TAP2 secondary structure predictions and experimentally determined membrane spanning segments (green and cyan) (1). Characteristic motifs and loops are indicated. The conserved glutamate residues of the X-loop are illustrated in red. The short (686 aa; PDB ID code gi:34638) and long TAP2 alleles [703 aa; PDB ID code gi:168985572 (gray)] are shown.

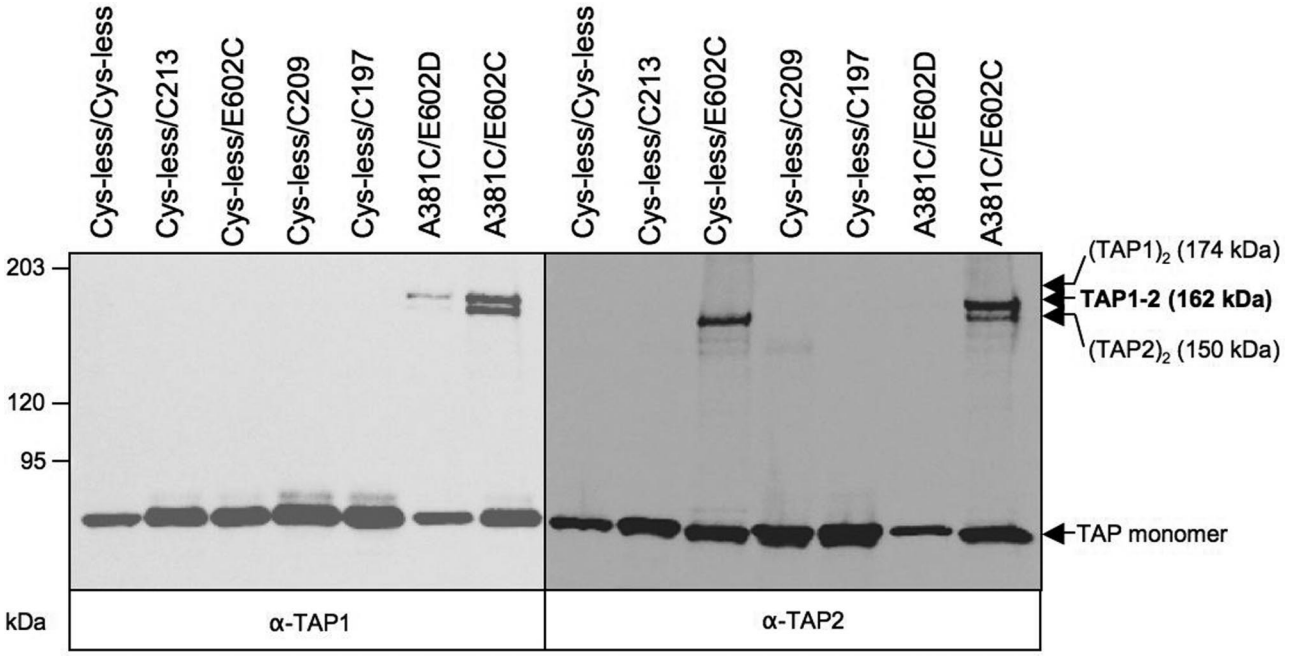

Fig. S2. Specific cross-linking between the cytosolic loops of TAP1 and the X-loop of TAP2. TAP-containing membranes (500 μg of total protein) were incubated in the presence or absence of 1 mM copper phenanthroline (CuPhe) for 1 min at 4 °C. Oxidative cross-linking was terminated by 10 mM each of *N*-ethylmaleimide (NEM) and EDTA. Samples were subjected to nonreducing 6% SDS/PAGE (20 μg of protein per lane) followed by immunoblotting against TAP1 and TAP2. The positions of the cross-linked TAP1–TAP2 (highlighted in bold), homodimeric $(TAP1)_2$ and $(TAP2)_2$ and monomeric TAP1 and TAP2 are indicated.

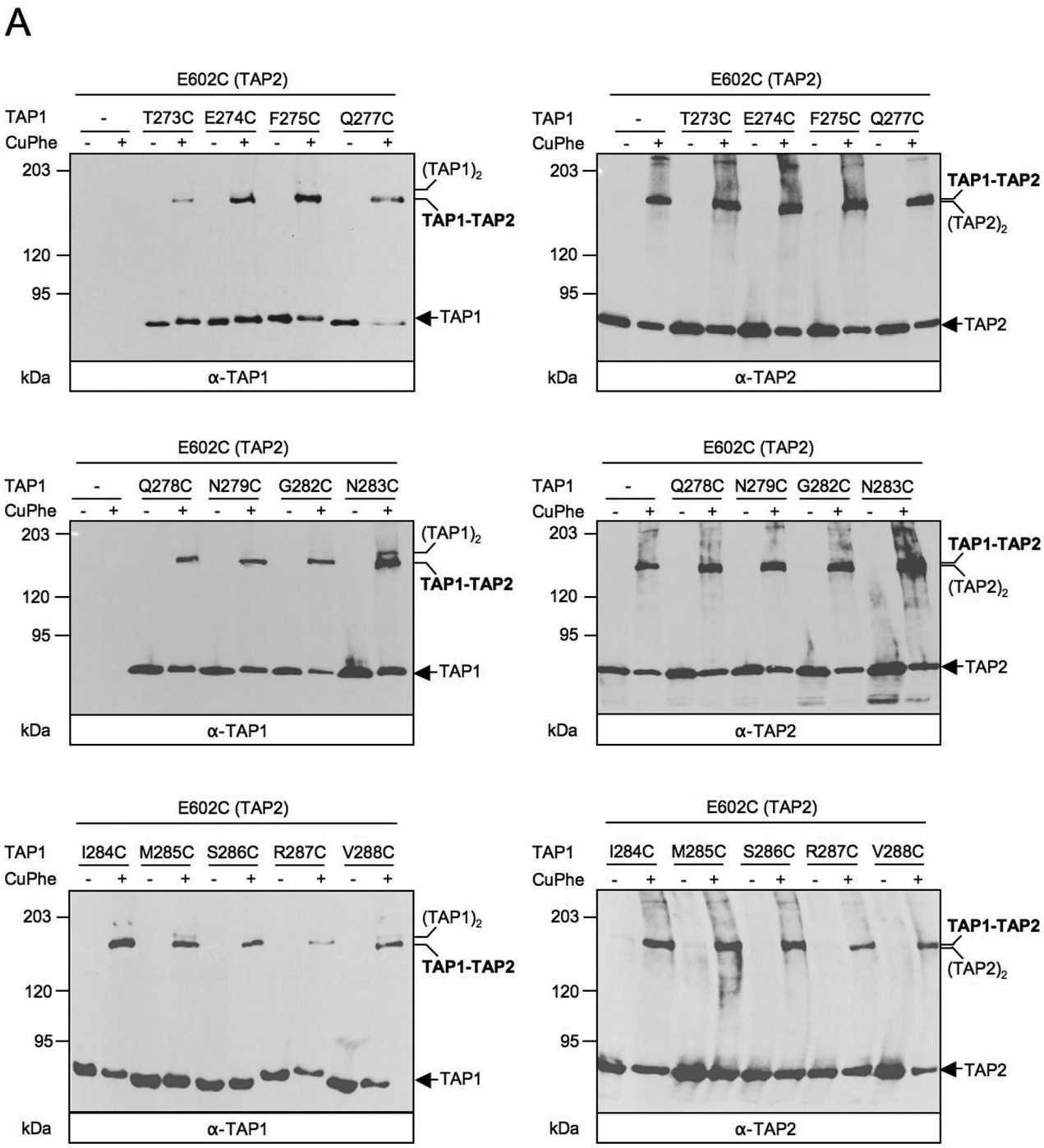

Fig. S3. Cysteine cross-linking between CL1 and CL2 of TAP1 and X-loop of TAP2. (*A* and *B*) The membranes (500 μg of protein) containing different single cysteine variants of the CL1 (*A*) and CL2 (*B*) of TAP1 and TAP2(E602C) were incubated in the presence or absence of 1 mM CuPhe for 1 min at 4 °C. Oxidative cross-linking was terminated by 10 mM each of NEM and EDTA. Samples were subjected to nonreducing 6% SDS/PAGE (20 μg of protein per lane) followed by immunoblotting against TAP1 and TAP2.

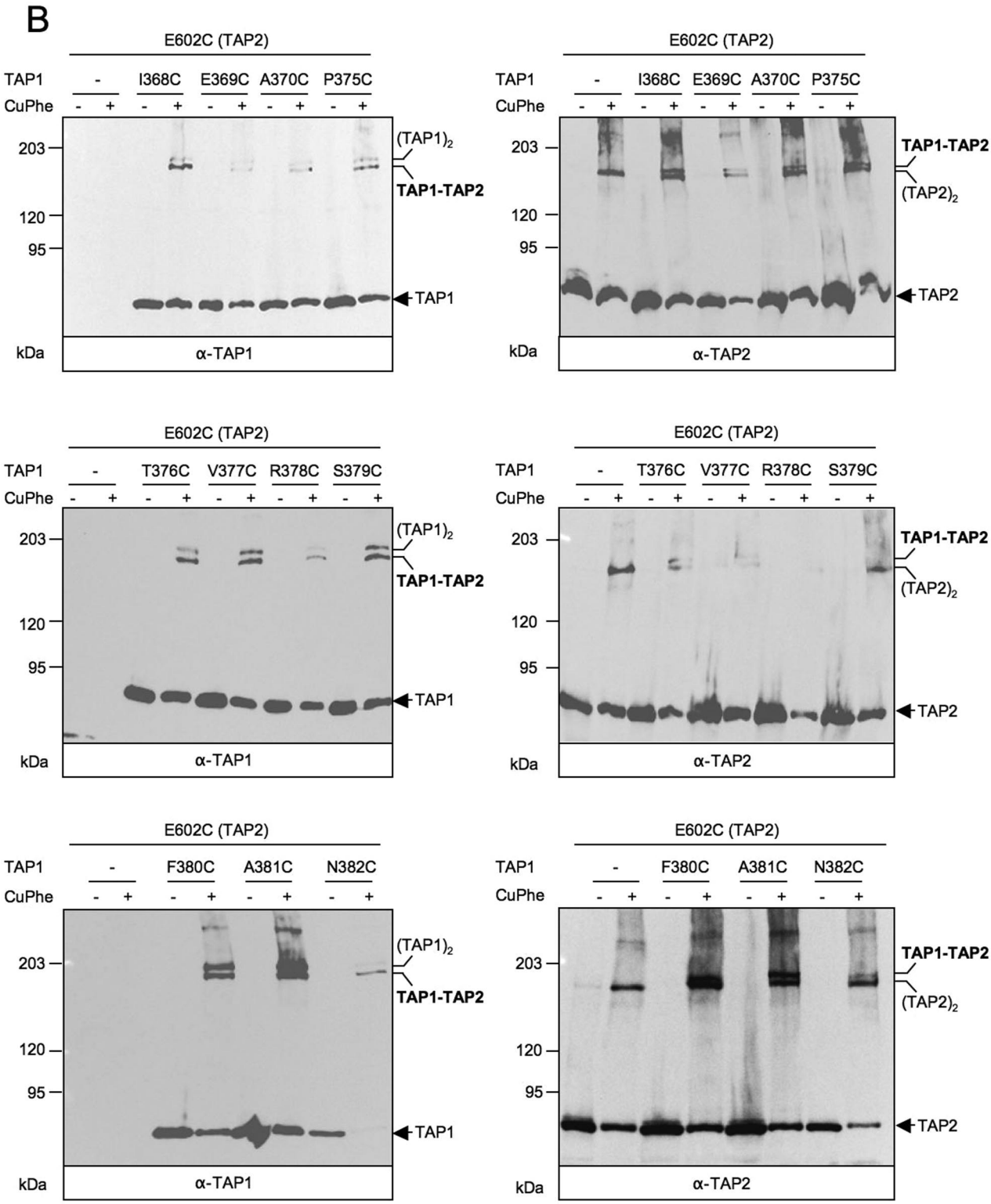

Fig. S3. continued.

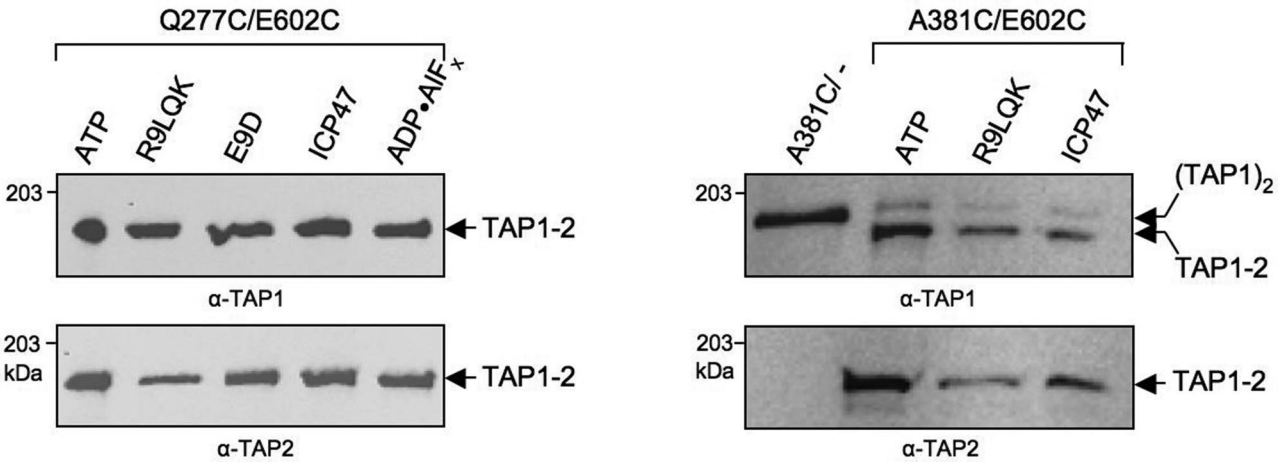

Fig. S4. Cross-linking efficiency between the X-loop and CL1 or CL2 remains stable at various stages of the transport cycle. TAP-containing membranes (500 μg of protein) were incubated with either 10 mM ATP, 10 μM R9LQK, 10 μM E9D (nonbinder), or 10 μM ICP47 for 25 min at 27 °C. For nucleotide trapping, TAP-containing membranes were preincubated with 1 μM RRYQKSTEL (R9LQK) and 5 mM ATP in the presence of 2.5 mM AlF_x for 25 min at 27 °C. Afterward, oxidative cross-linking was initiated in the presence of 1 mM CuPhe for 1 min at 4 °C. Oxidative cross-linking was terminated by 10 mM each of NEM and EDTA. After metal affinity capture of TAP, cross-linked products were analyzed by nonreducing 6% SDS/PAGE followed by immunoblotting against TAP1 and TAP2. The positions of the cross-linked heterodimeric TAP1–2 and homodimeric $(TAP1)_2$ are indicated.

Table S1. CL/X-loop distances in different TAP1/2 models

TAP1/2 model based on	CL1 C_α distances for residues 277–602, Å	CL2 C_α distances for residues 381–602, Å
Sav1866 (PDB ID code 2HYD)	7.7	20.5
ADP-vanadate MsbA (PDB ID code 3B5Z)	7.0	21.0
closed apo MsbA (PDB ID code 2B5X)	26.5	25.6
open apo MsbA (PDB ID code 2B5W)	63.1	26.0